

## Response of lower limb in full-scale car–pedestrian low-speed lateral impact – influence of muscle contraction

Anurag Soni<sup>a</sup>, Anoop Chawla<sup>a\*</sup>, Sudipto Mukherjee<sup>a</sup> and Rajesh Malhotra<sup>b</sup>

<sup>a</sup>Department of Mechanical Engineering, Indian Institute of Technology, New Delhi 110016, India; <sup>b</sup>Department of Orthopaedics, All India Institute of Medical Sciences, New Delhi 110016, India

(Received 21 June 2008; final version received 24 January 2009)

This paper investigates the effect of muscle contraction on lower extremity injuries in car–pedestrian lateral impact. A full-body pedestrian model with active muscles has been developed. Finite element simulations have then been performed using the full-body model and front structure of a car. Two pre-impact conditions, that of a symmetrically standing pedestrian, representing a cadaver and an unaware pedestrian, have been simulated. Stretch-based reflexive action was included in the simulations for an unaware pedestrian. The results show that due to muscle contraction (1) peak strain in all the knee ligaments reduces, (2) von Mises stresses in tibia and fibula increase and may fail and (3) knee joint effective stiffness increases by 58% in lateral bending.

**Keywords:** A-LEMS; lower extremity model; finite element model; dynamic simulation; muscle contraction; standing posture; car–pedestrian impact; knee injury

### Introduction

Pedestrians constitute 65% of the 1.17 million people killed annually in road traffic accidents worldwide [24]. Epidemiological studies on pedestrian victims have indicated that together with the head, the lower extremity is the most frequently injured body region [5, 15]. Pedestrian Crash Data Study (PCDS) [5] reports that passenger cars have the biggest share in vehicle–pedestrian accidents. Further, the front bumper is the major source of injury to the lower extremity when injuries are caused by a vehicle [15]. This has posed an interesting challenge for vehicle designers to design pedestrian-friendly car front structures. To devise effective pedestrian protection systems, it is essential to understand the injury mechanism.

So far the lower limb injury mechanism in car–pedestrian crashes has been studied through tests on human cadaver specimens [2,6–9] and simulations using validated passive finite element (FE) models [3,13,17, 18, 20, 21]. However, the major shortcoming in these existing experimental and computational studies is that they do not account for muscle action. Therefore, effects of pre-crash muscle contraction on the response of lower limbs in car–pedestrian crashes remains unclear.

Of late, Soni et al. [20] have investigated the probable outcome of muscle contraction using a lower limb (single-leg) FE model with active muscles (A-LEMS). More recently, Chawla et al. [4] have performed a study using the A-LEMS and reported that with muscle contraction, the

risk of knee ligament failure is likely to be lower than that predicted through the cadaver tests or simulations with the passive FE models. However, in these studies a single-leg model (A-LEMS) has been used and the geometry of the upper body has not been considered. In addition, an impactor of mass 20 kg is used which is much lighter than a physical car. As a result, the conditions simulated in these studies may not correspond to an actual crash.

The present study extends our earlier studies to investigate the effect of muscle contraction on the response of lower limbs in a full-scale car–pedestrian lateral collision using FE simulations. For this, a single-leg model (A-LEMS) has been extended to a full-body model. The real-world car–pedestrian lateral impact has been simulated using the full-body model and front structures of a validated car FE model. A pedestrian standing symmetrically with legs positioned in a side-by-side stance has been simulated for two pre-impact pedestrian conditions, i.e. with deactivated muscles and with activated muscles mimicking an unaware pedestrian. Stretch-based involuntary reflex action has been included in the simulation for an unaware pedestrian. Strains in knee ligaments, von Mises stresses in bones and tibia displacements for two levels of muscle activation are then compared to assess the effect of muscle contraction.

### Description of A-LEMS

In the present study, A-LEMS has been used. The A-LEMS includes 42 muscles modelled as 1-D bar elements, in

\*Corresponding author. Email: achawla@mech.iitd.ernet.in

addition to the passive structures such as the cortical and the spongy parts of the femur, tibia, fibula, and the patella. The cortical part of the bones is modelled by shell elements, while the spongy part is modelled by solid elements. Apart from these, passive muscle response and skin are also modelled using solid elements and membrane elements respectively. Knee ligaments, anterior cruciate ligament (ACL), posterior cruciate ligament (PCL) and lateral collateral ligament (LCL) have been modelled using solid elements. Because of a smaller thickness compared to the width, the medial collateral ligament (MCL) has been modelled using the shell elements. The articular capsule, i.e. 'knee capsule', which encloses the knee joint and maintains joint integrity, has also been included in this model.

Since all the available data is for cadaver tests, the passive version of the A-LEMS was validated against loading and boundary conditions reported in [8, 9, 10]. These validation results have been presented in detail in [20]. The passive model correctly reproduces impactor forces, knee kinematics and ligament failures reported from the experiments. Forty-two active muscles, modelled as 1-D bar elements with the Hill material model, are subsequently activated to simulate the effect of muscle contraction. Details regarding activation levels and Hill model parameters (such as maximum muscle force ( $F_{max}$ ), optimum muscle length ( $L_{opt}$ ), maximum contraction velocity ( $V_{max}$ ), fraction of fast fibres ( $C_{fast}$ ) and initial activation level ( $N_a$ ) are available in [19, 20].

### Full-body model development

In the present study, a full-body pedestrian model with active muscles in both legs has been developed. For this the A-LEMS [20] was adopted as the base model. In order to extend the A-LEMS to a full-body model, an additional leg and the upper extremity were introduced. FE mesh of the additional leg was obtained through mirror transformation of the existing lower extremity mesh in the A-LEMS about the sagittal plane using HYPER-MESH<sup>TM</sup>. Material properties of each mirrored segment and the contact definitions between them were kept identical as in the A-LEMS. As a result, a two-legged FE model (legs positioned symmetrically in a side-by-side stance) with 42 muscles in each leg was obtained.

Though the focus in the current study is to investigate the response of lower extremity, the upper extremity is important to take into account the effects of mass and moment of inertia of the upper body. Therefore, it has been decided to model upper extremity segments using geometrically accurate rigid body definitions. Hence, the upper extremity segments in standard H-III dummy models available with PAM-CRASH<sup>TM</sup> have been separated and integrated with the two-legged FE model.

The assembled full-body model thus obtained was then aligned in a symmetric standing posture of the pedestrian

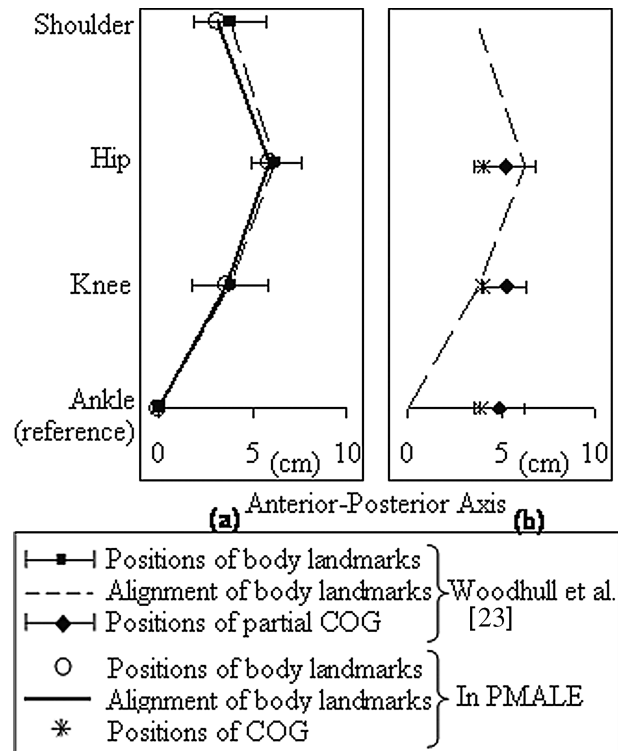


Figure 1. Comparison of (a) alignment of body landmarks and (b) partial COG positions of the PMALE segments with the corresponding positions reported in [23].

whose legs are in a side-by-side stance. It was ensured that pre-impact loading conditions with respect to the forces and moments at the knee joint corresponded to the conditions for a symmetrically standing pedestrian. Two aspects of the alignment have been considered here: (1) anterior-posterior position of the knee joint, the hip joint and the shoulder joint relative to the ankle joint and (2) anterior-posterior position of partial centre of gravity (COG) above the knee and the hip joints.

Relative positions of the body segments required to define the alignment of the symmetric standing posture were taken from [23]. A series of FE simulations were performed with the assembled full-body model to acquire a statically competent alignment between its segments. We will refer to the aligned full-body model as Pedestrian Model with Active Lower Extremity (PMALE). Figure 1 shows the comparison of the alignment of body landmarks (Figure 1a) and positions of partial COG (Figure 1b) of the PMALE segments with the corresponding positions given in [23].

### Simulations for standing posture

#### Simulation set-up

Figure 2 shows the simulation set-up used in the present study. Here, the real-world car-pedestrian impact has been reproduced using the PMALE and front structures of a validated car FE model. PMALE is configured as standing

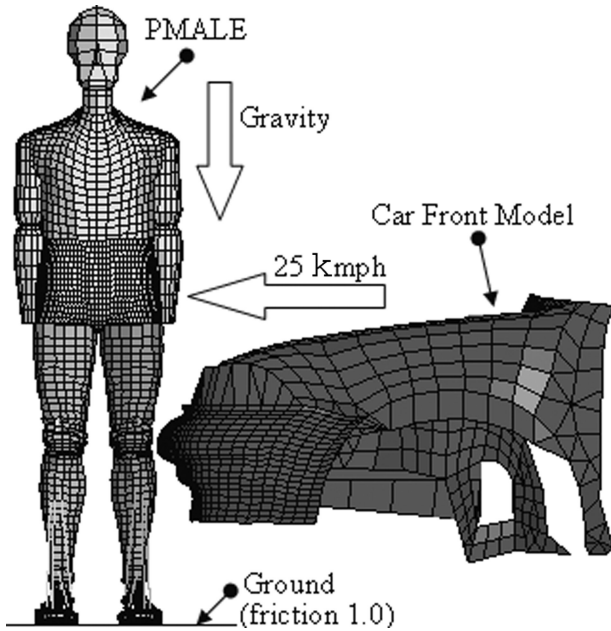


Figure 2. Simulation set-up used in the present study.

freely with legs in a side-by-side stance on a rigid plate in a gravity field. The coefficient of friction between the shoes and the ground is set to 1.0 as suggested for grooved rubber on road [12].

Pedestrian accident studies [5, 16] have shown significant incidence of bone fracture for high-speed impacts. Since bone fracture unloads the knee joint, we decided to simulate low-speed impact. On the basis of PCDS [5], which reports a range of 20–30 kmph for low-speed impacts, an impact speed of 25 kmph was selected. A car model with a total mass of 1158 kg (mass of the front structure is 355 kg, and 803 kg is modelled as the added mass to account for the remaining car structures) was thus propelled towards the PMALE to impact its left leg laterally. The PMALE was placed in front of the car model to interact with the middle of the bumper, with the bumper height above the ground such that it corresponds to the car rolling on its tyres.

In the present study, each simulation was run for 100 ms. For the initial 50 ms (stabilisation duration), the PMALE was allowed to stabilise under gravity. The car model came in contact with the PMALE only at the end of the stabilisation duration (i.e. after the first 50 ms).

### **Pedestrian pre-impact conditions**

Two pre-impact pedestrian conditions, i.e. with deactivated muscles and with activated muscles (including reflex action), for an unaware pedestrian have been simulated in the present study. We call these conditions cadaveric and reflex conditions respectively. These conditions differ in terms of initial activation levels in muscles and whether the re-

flex action is enabled. By enabling the reflex action for a muscle, the activation level in that muscle rises with time during the simulation; this increases the force produced by that muscle.

*Cadaveric condition:* In this condition, a freely standing cadaver was simulated. To model a cadaver in FE simulation, all the muscles in PMALE were assigned the minimum value of 0.005 as an initial activation level. The reflex action was also disabled. As a result, in this condition, activation levels in each muscle remained at the minimum value (i.e. 0.005) for the entire duration of the simulation. Therefore, all the muscles function at their minimum capacity.

*Reflex condition:* In this condition, a symmetrically standing pedestrian who is unaware of an impending crash has been simulated. To model an unaware standing pedestrian, activation levels for maintaining the stability of the standing posture of a pedestrian in gravity field are the input. Kuo and Zajac [11] report activation levels in lower limb muscles for near-erect standing posture with flexion/extension about the ankle joint (i.e. ankle strategy) keeping other joints motionless. It is important to highlight here that standing posture is not a stable posture. While standing erect, the human body sways back and forth in sagittal and frontal plane about the ankle joint. In the present study, muscle activation levels for the standing posture with ankle in extension were selected. These activation values are listed in Table 1. Thus, the chosen set of muscle activation levels would be able to correctly represent the normal standing posture of a pedestrian.

A stretch-based involuntary reflex action has also been enabled in this condition. For enabling the reflex, a threshold value of elongation is to be defined in the Hill material card of a muscle. When the elongation in muscle crosses the threshold value, the stretch reflex in a muscle gets activated. However, the increase in muscle force starts only after a certain time known as reflex time. This delay between the activation of stretch reflex and the onset of increase in muscle force represents the time taken by the signal to travel through the central nervous system circuitry (muscle-spinal cord-muscle). A delay of 20 ms was assigned to all the muscles in PMALE [1]. This mimics the ability of live muscle to respond to a small stretch produced by an outside agency. In medical terms this kind of reflex action is known as ‘stretch reflex’ [22].

### **Data analysis**

Two nodes each in the femur and tibia were selected (Figure 3a) to compute the relative tibia displacements and the knee joint angles. Figure 3b shows the sign conventions used in the current study. Springs of very low stiffness were modelled on each knee ligament to calculate ligament strains. Element elimination approach has been enabled to simulate the failure in the ligaments and the bones. A

Table 1. Values of muscle parameters used to define Hill muscle cards of 42 muscles.

Lower extremity muscles	$F_{max}$ (N)	$L_{opt}$ (m)	$C_{fast}$	$aV_{max}$	$N_a$
Vastus lateralis	1871	0.084	0.52	5.85	0.005
Vastus intermedius	1365	0.087	0.5	5.10	0.005
Vastus medialis	1294	0.089	0.53	5.36	0.005
Rectus femoris	779	0.084	0.619	5.55	0.005
Soleus	2839	0.03	0.25	2.67	1 <sup>a</sup>
Gastrocnemius medialis	1113	0.045	0.518	5.74	1 <sup>a</sup>
Gastrocnemius lateralis	488	0.064	0.518	5.69	1 <sup>a</sup>
Flexor hallucis longus	322	0.043	0.5	5.17	0.005
Flexor digitorum longus	310	0.034	0.5	4.58	0.005
Tibialis posterior	1270	0.031	0.5	4.65	1 <sup>a</sup>
Tibialis anterior	603	0.098	0.27	3.28	0.5 <sup>a</sup>
Extensor digitorum longus	341	0.102	0.527	5.31	0.005
Extensor hallucis longus	108	0.111	0.5	4.32	0.005
Peroneus brevis	348	0.05	0.375	4.59	1 <sup>a</sup>
Peroneus longus	754	0.049	0.375	4.35	0.005
Peroneus tertius	90	0.079	0.375	4.76	0.005
Biceps femoris (LH)	717	0.109	0.331	3.55	1 <sup>a</sup>
Biceps femoris (SH)	402	0.173	0.331	3.91	1 <sup>a</sup>
Semimembranosus	1030	0.08	0.5	5.61	1 <sup>a</sup>
Semitendinosus	328	0.201	0.5	4.76	1 <sup>a</sup>
Piriformis	296	0.026	0.5	5.71	0.005
Pectineus	177	0.133	0.5	4.62	0.005
Obturatorius internus	254	0.049	0.5	5.71	0.005
Obturatorius externus	109	0.030	0.5	5.71	0.005
Gracilis	108	0.352	0.5	5.13	0.005
Adductor brevis 1	286	0.133	0.5	5.17	0.005
Adductor brevis 2	286	0.133	0.5	5.22	0.005
Adductor longus	418	0.138	0.5	4.69	0.5 <sup>a</sup>
Adductor mangus 1	346	0.087	0.416	5.07	0.005
Adductor mangus 2	444	0.121	0.416	5.07	0.005
Adductor mangus 3	155	0.131	0.416	5.07	0.005
Glutaeus maximus 1	382	0.142	0.476	5.53	0.005
Glutaeus maximus 2	546	0.147	0.476	5.53	0.005
Glutaeus maximus 3	368	0.144	0.476	5.53	0.005
Glutaeus medius 1	546	0.054	0.5	5.71	0.005
Glutaeus medius 2	382	0.084	0.5	5.71	0.005
Glutaeus medius 3	435	0.065	0.5	5.71	0.005
Glutaeus minimus 1	180	0.068	0.5	5.71	0.005
Glutaeus minimus 2	190	0.056	0.5	5.71	0.005
Glutaeus minimus 3	215	0.038	0.5	5.71	0.005
Sartorius	104	0.579	0.504	5.03	0.005
Tensor fasciae latae	155	0.095	0.5	5.71	1 <sup>a</sup>

<sup>a</sup>These values of muscle activation levels have been taken from [10].

transverse plane has been defined at the knee joint of the impacted leg (i.e. left leg of PMALE) to calculate the knee-bending moment in the simulations. Knee kinematics, strain time history of each knee ligament, von Mises stress contours in bones and lateral bending stiffness of knee joint of the impacted leg, i.e. the left leg of the PMALE, have been recorded from the simulations. Response in cadaveric and reflex conditions was then compared to determine the role of muscle contraction.

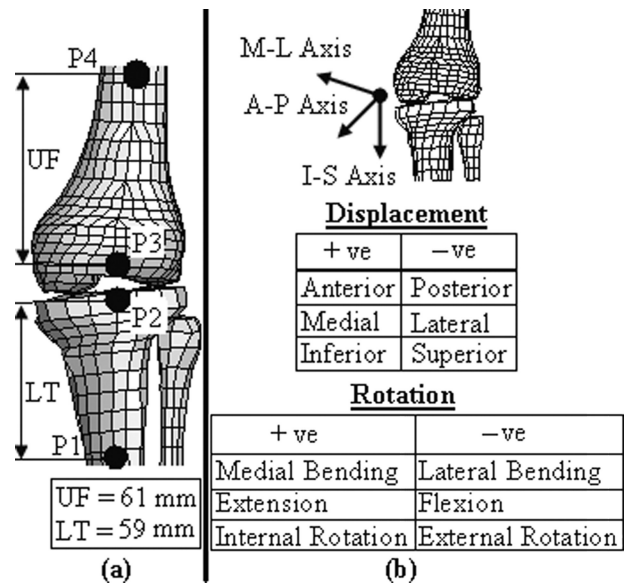


Figure 3. (a) Locations of nodes at which nodal time histories have been obtained in the current study and (b) sign conventions used to calculate relative tibia movements.

**Results**

In the present study, two simulations, each of 100 ms duration, have been performed. For the first 50 ms (stabilisation duration), PMALE has been stabilised under gravity load in both the simulations. At the end of the first 50 ms, the car front impacts the left leg of the stabilised PMALE. Knee joint contact force, knee kinematics, and von Mises stresses in bones and ligament strains have been recorded from the simulations to assess the effect of muscle contraction. Results presented here are for the impact duration, and the initial time (i.e. 0 ms) corresponds to the time of impact.

**Knee joint contact force**

Figure 4 compares the contact force time history calculated at the knee joint (i.e. between tibia plateau, meniscus and femur condyle) of the impacted leg (left leg of PMALE)

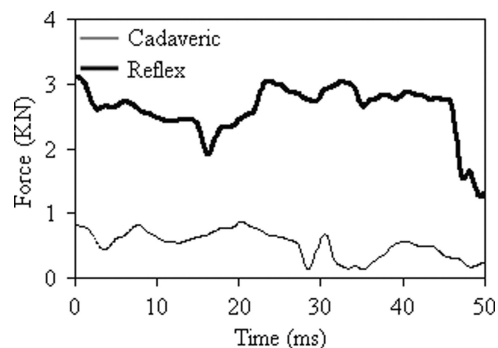


Figure 4. Comparison of knee contact force–time history.

for both cadaveric and reflex conditions. It is apparent that due to the muscle action in reflex condition, contact force at the knee joint remains significantly higher (ranged between 1.3 and 3.1 KN) as compared to the cadaveric condition (ranged between 0.79 and 0.25 KN) in the entire duration of the simulation. This indicates that in the reflex condition, active muscle forces pull the tibia towards the femur and therefore the knee joint remains tightly enclosed. This eventually results in higher compressive forces between the tibia plateau, the meniscus and the femur condyles in the reflex condition as compared to the cadaveric condition.

### Knee joint kinematics

Linear and angular tibia displacement time histories relative to femur for both cadaveric and reflex conditions are compared in Figures 5 and 6 respectively. It is evident that active muscle forces have significantly affected the knee joint kinematics in reflex condition as compared to the cadaveric condition.

In simulations for both cadaveric and reflex conditions, the car front impacts the lateral side of the knee joint of the left leg. As a result, both the tibia and the femur at the knee level are forced to move in the medial direction. Due to this, the relative medial tibia displacement (Figure 5b) and the medial knee-bending angle (Figure 6b) increase for the initial 10–13 ms. After 13 ms, the momentum of the car front further pushes the tibia and the femur at the left knee joint

to move together in the medial direction. As a result, the medial knee-bending angle (Figure 6b) increases further. However, the relative medial tibia displacement (Figure 5b) remains nearly unaltered till 28 ms.

Later, after around 28–30 ms, the left foot loses contact with the ground. Since the left leg is rigidly attached to the massive upper body via the pelvis at the femur end, this event frees the lower leg to move away from the femur in the inferior direction and eventually sets the left leg in motion. This results in a sudden increase in the inferior tibia displacement (Figure 5c) and the medial bending (Figure 6b) at around 28 ms.

By 30 ms, the moving left leg gradually establishes contact with the medial side of the right leg, and the contact force between them peaks after around 38–40 ms. During this interaction (30–40 ms), the right leg along with the friction at the right foot inhibits the motion of the left leg. However, the inferior tibia displacement (Figure 5c) and the medial bending (Figure 6b) keep on increasing and reach a peak at around 40 ms. After 40 ms, the car front carries away both the legs together in the lateral direction. Due to this, the right leg also comes into motion and then rotates the pelvis. As the pelvis is rigidly connected to the upper body at the sacrum, this event eventually sets the medial rotation in the upper body. As a result, during 40–50 ms, medial tibia displacement (Figure 5b) suddenly shoots up, whereas the inferior tibia displacement (Figure 5c) and medial knee bending (Figure 6b) become constant.

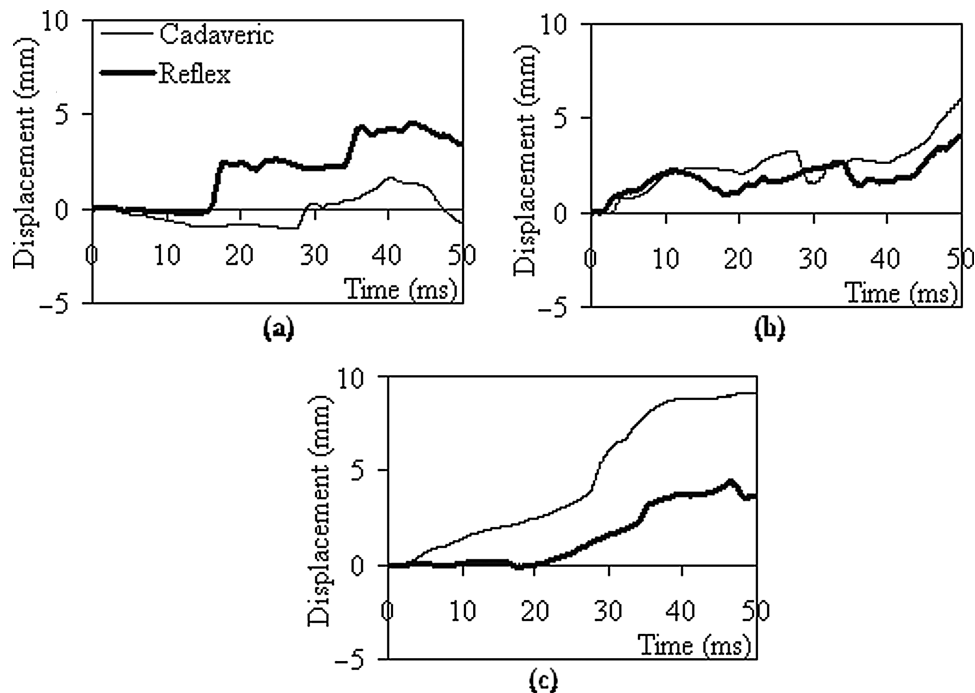


Figure 5. Comparison of relative tibia displacements of the impacted leg (i.e. left leg) in (a) anterior-posterior, (b) medial-lateral and (c) inferior-superior directions.

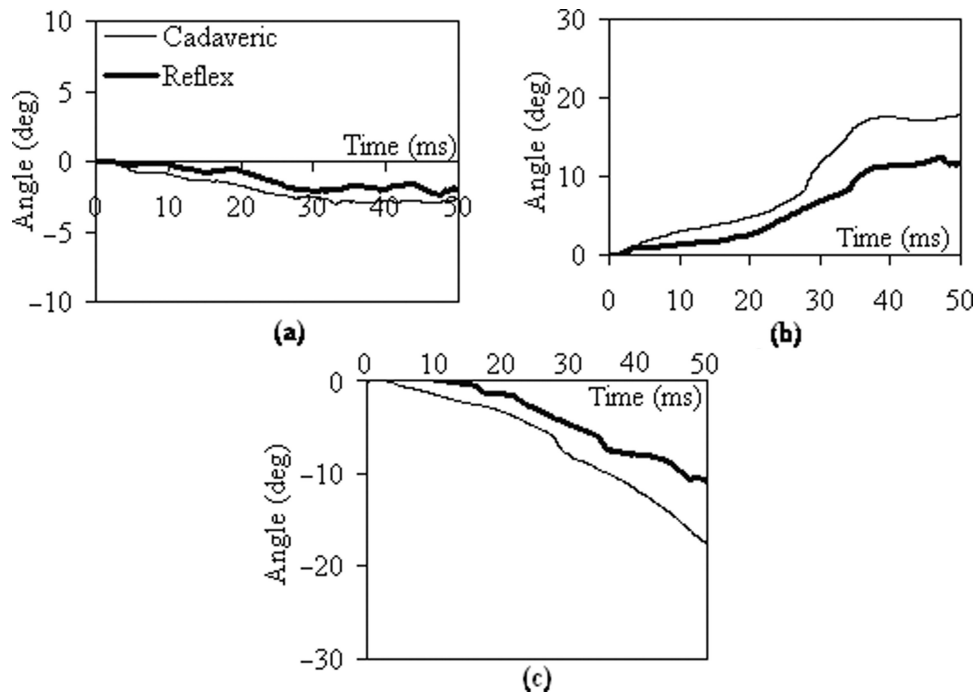


Figure 6. Comparison of relative knee angles of the impacted leg (i.e. left leg): (a) extension-flexion, (b) medial-lateral bending and (c) internal-external rotations.

In the reflex condition, active muscle forces pull the tibia towards the femur. As a result, the inferior tibia displacement (Figure 5c), the knee external rotation (Figure 6a) and the medial bending angle (Figure 6b) are significantly reduced in the reflex condition as compared to the cadaveric condition. The peak inferior tibia displacement reduces by a factor of 2, the peak knee external rotation by a factor of 1.62 and the peak medial bending angle by a factor of 1.45. However, the peak value of the anterior tibia displacement (Figure 5a) is increased by 2.67 times in the reflex condition as compared to the cadaveric condition. This could be attributed to the higher active force in the gastrocnemius muscles in the reflex condition (peak value 1200 N) as compared to the cadaveric condition (peak value 40 N), which eventually forces the femur at the knee joint to move in the posterior direction causing higher anterior tibia displacement in the reflex condition.

### Strain in knee ligaments

Figure 7 illustrates the calculated strain time history in knee ligaments of the impacted leg (i.e. left leg of the PMALE) for both cadaveric and reflex conditions. It is evident that strains in knee ligaments reduce significantly in the reflex condition as compared to the cadaveric condition.

**ACL:** Figure 7a compares the strain time history in ACL for both the conditions. It is observed that till 16 ms, ACL remained nearly unstrained in both the conditions.

Then, in the reflex condition, strain in ACL suddenly increased to approximately 2% and remained higher than in the cadaveric condition (1.5%) till 29 ms. This sudden rise in ACL strain can be attributed to the increased anterior tibia displacement (Figure 5a) in the reflex condition as compared to the cadaveric condition. After 29 ms, strain in ACL is observed to be higher in the cadaveric condition (peak value 6.51% at 40 ms) than in the reflex condition (peak value 4.95% at 44 ms). This is attributed to higher inferior tibia displacement (i.e. away from femur) in the cadaveric condition (Figure 5c). It is observed that peak strain value in ACL dropped by a factor of 1.3 in the reflex condition as compared to the cadaveric condition.

**PCL:** Strain time history in PCL is compared for both the conditions in Figure 7b. It is observed that reduction in strain due to muscle action is more prominent in PCL than in the ACL. In the cadaveric condition, strain in PCL reached up to 4.03%, whereas in the reflex condition it remained nearly at 0% for the entire duration of the simulation. Relative displacement of tibia in the inferior direction is the major source of strain in the PCL. Figure 5c illustrates that in both cadaveric and reflex conditions, the tibia is moving away from the femur. However, active muscle forces in the reflex condition have pulled the tibia towards the femur and therefore tibia displacement in the inferior direction (i.e. away from the femur) has reduced (Figure 5c). This has slackened the PCL in the reflex condition.

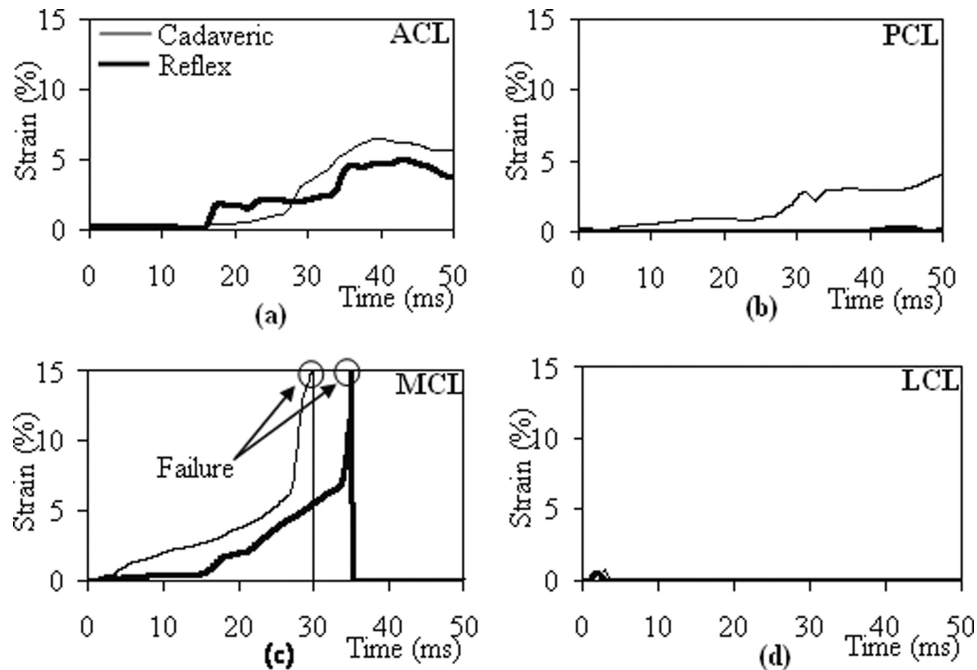


Figure 7. Comparison of strain–time history in knee ligaments: (a) ACL, (b) PCL, (c) MCL and (d) LCL of the impacted leg (i.e. left leg).

**MCL:** Strain in MCL for both the conditions is shown in Figure 7c. It is observed that peak MCL strain has reached the ligament failure limit of 15% in both the conditions. However, in comparison to the cadaveric condition (30 ms), failure is delayed by 5 ms in the reflex condition (35 ms). The delay in MCL failure can be attributed to the combined effect of reduced inferior tibia displacement (Figure 5c) and medial knee bending (Figure 6b) in the reflex condition as compared to the cadaveric condition. Rupture in MCL in both the simulations agrees with the results of statistical analysis of real-world accidents in which MCL is reported as the most frequently injured knee ligament [14].

**LCL:** It is observed that strain in LCL (Figure 7d) remains below 1% in both the conditions. This can be ascribed to the lateral impact which forces the tibia to bend medially and consequently keeps the LCL slackened.

#### Von Mises stresses in bones

Figures 8 and 9 show the von Mises stress distribution on the bones of the impacted leg (i.e. left leg). It is apparent that stresses in bones increased significantly in the reflex condition as compared to the cadaveric condition.

von Mises stress distribution on femur and tibia at the knee joint of the impacted leg at different stages of the simulation for both cadaveric and reflex condition is compared in Figure 8. It is observed that in the reflex

condition (Figure 8b), stresses in the bones (especially at the femur lateral condyle region) are significantly higher (between 104 and 138.1 MPa), and larger areas of the bones are stressed as compared to the cadaveric condition (Figure 8a). This can be attributed to the higher compressive forces (shown in Figure 4) between the tibia plateau and the femur condyle caused by the muscle pull in the reflex condition.

Later, at 48 ms in the reflex-enabled situation (Figure 9a), the medial sides of the mid tibia and fibula were stressed to their ultimate stress limit (138.1 MPa) and consequently fractured in the simulation. However, in the cadaveric condition (Figure 9b) stress in tibia and fibula remained below the failure limits.

#### Knee lateral bending stiffness

Figure 10 compares the knee lateral bending moment and the angle response of the impacted leg for both cadaveric and reflex conditions. Peak bending moment is found to be significantly higher in the reflex condition (135 Nm) than in the cadaveric condition (96 Nm). Knee-bending angle (Figure 6b) at the time of MCL failure decreased by approximately  $1^\circ$  in the reflex condition ( $10.2^\circ$ ) as compared to the cadaveric condition ( $11.3^\circ$ ). Linear regression was performed on the bending moment – angle response shown in Figure 10 to obtain a representative lateral bending stiffness of the knee joint. It is found that lateral bending stiffness

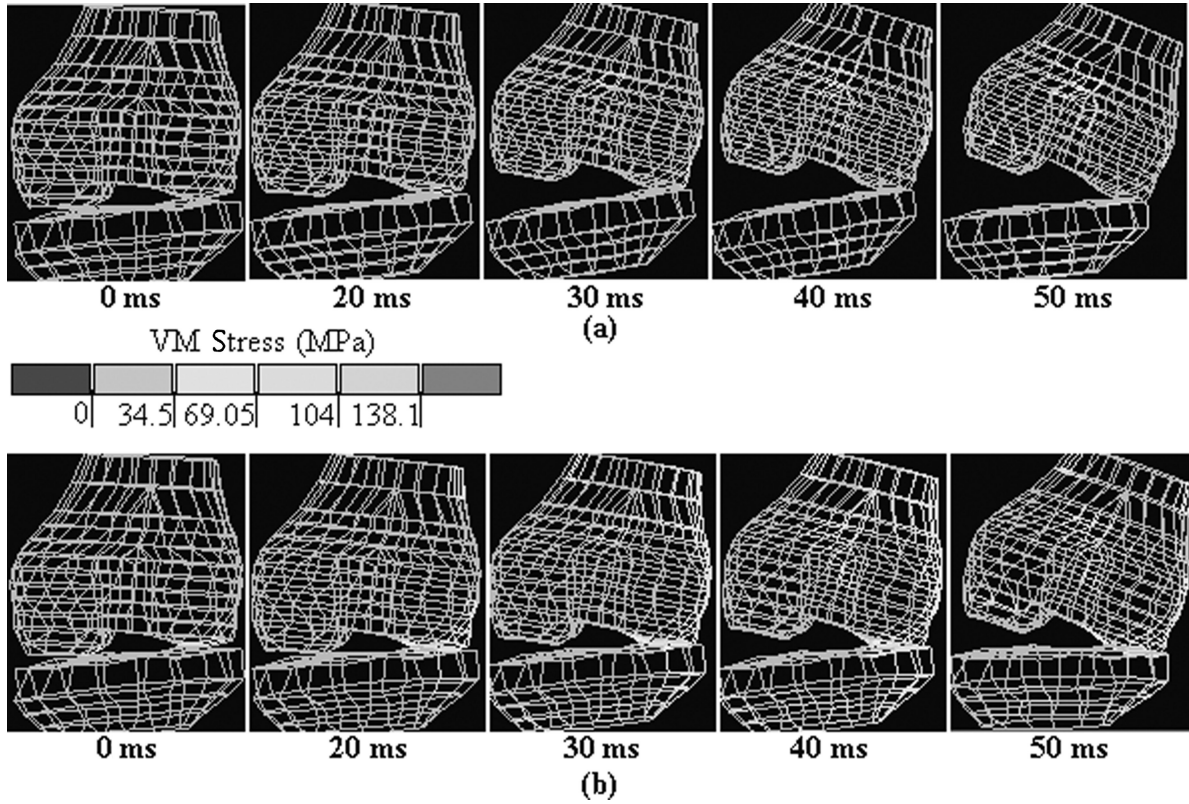


Figure 8. Comparison of von Mises stress distribution on bones at the knee joint of the impacted leg (i.e. left leg) at different stages of the simulations for (a) cadaveric and (b) reflex conditions (meniscus and other soft tissues are not shown here).

of the knee joint significantly increased by approximately 58% in the reflex condition (18.93 Nm/deg,  $R^2 = 0.8849$ ) as compared to the cadaveric condition (11.99 Nm/deg,  $R^2 = 0.986$ ).

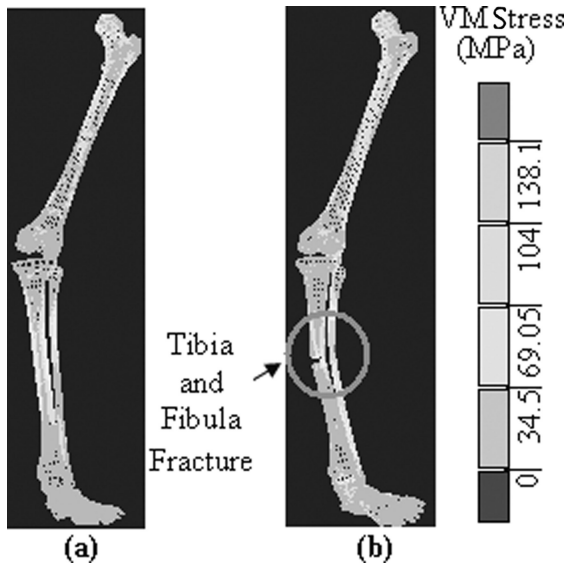


Figure 9. Comparison of von Mises stress distribution on femur, tibia and fibula of the impacted leg (i.e. left leg) at 48 ms for (a) cadaveric and (b) reflex conditions.

**Discussion**

In the present study, effects of active muscle forces on the response of lower extremity in a full-scale car-pedestrian lateral impact have been investigated using FE simulations. Two pre-impact conditions, representing a cadaver and an unaware pedestrian, have been considered. It is observed that active muscle forces have significant effects on the lower extremity loading. Based on these FE simulations,

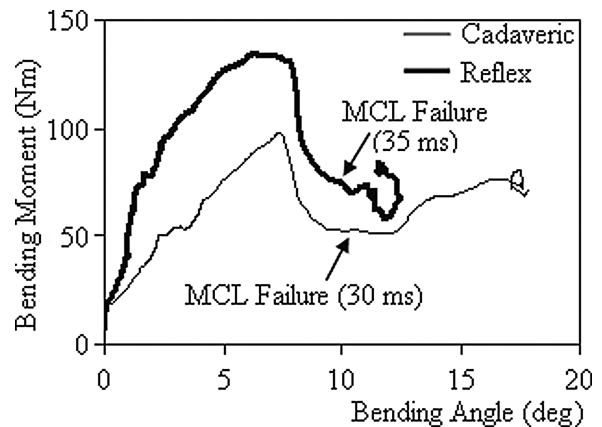


Figure 10. Comparison of knee-bending moment – angle response of the impacted leg.

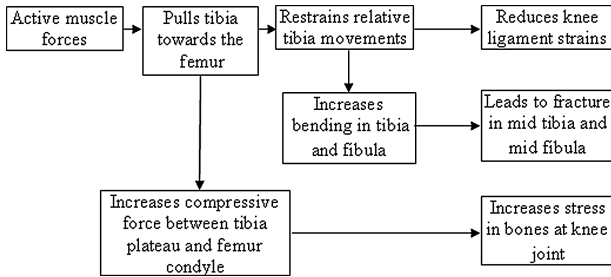


Figure 11. Role of active muscle forces.

the role of active muscle forces has been summarised in Figure 11.

Active muscle forces pull the tibia close to the femur and hence hold the knee joint tightly. The tightly enclosed knee joint has two effects:

- On one hand, it restricts the relative movement between the tibia and the femur and consequently alters the post-impact knee kinematics. This eventually reduces the strain in knee ligaments. The restricted relative tibia movements at knee level along with friction at the foot of the axially compressed leg restrain lower leg motion. This increases the bending in the tibia and fibula and results in fracture.
- On the other hand, muscle pull causes higher compressive forces between the tibia plateau and the femur condyles, which results in higher stresses in these bones in the knee region.

The present study indicates that active muscles have potentially important effects on lower extremity injuries during a car–pedestrian lateral impact and FE simulations can be a viable tool to study these effects. However, to correctly model active muscle forces in the simulations, activation levels in the muscles representing the pre-crash pedestrian conditions are required as an input. This signifies the future direction of pedestrian safety research, since unlike car occupants, pedestrian crashes occur in a variety of postures (like stationary, walking, running or jogging). For different human body postures, the central nervous system either recruits entirely different sets of muscles or activates the same set of muscles at different levels. Therefore, it becomes essential to quantify patterns of pedestrian pre-crash conditions in terms of activation levels, which can then be used as an initial input to study muscle effects on lower extremity loading for a pedestrian undergoing crash in different postures.

## Conclusions

In the present study, a full-body pedestrian model (named as PMALE) with 42 active muscles in each leg has been developed. PMALE is then used to investigate the effects

of active muscle forces on the response of lower extremity in a car–pedestrian lateral impact. Differences in response between a cadaver and an unaware pedestrian who is standing symmetrically with legs in a side-by-side stance (with active muscles) have been studied. To assess the effect of muscle activation, knee joint contact force, strains in knee ligaments, VonMises stress in bones and knee lateral bending moment – angle response of the impacted leg (i.e. left leg of the PMALE) have been compared. The following conclusions can be drawn:

- (1) Active muscle forces in the reflex condition pull the tibia close to the femur and eventually alter the knee kinematics.
- (2) In the present study, peak strains in all knee ligaments were found to be lower in the reflex condition (with active muscles). This reinforces our previous findings that the risk of ligament failure in real-life crashes is likely to be lower than that predicted through cadaver tests or simulations.
- (3) MCL failed, whereas LCL remained nearly unstrained. This implies that in lateral impacts, MCL could be considered as the most vulnerable ligament and LCL as the safest.
- (4) Increased stresses in bones at the lateral side of the knee joint and failure occurred at mid tibia and mid fibula in the reflex condition. It leads to the conclusion that chances of bone fracture increase with muscle contraction.
- (5) Knee lateral bending stiffness increased by 58% in the reflex condition. This suggests that due to muscle contraction, the knee joint becomes stiffer in lateral bending.

## Acknowledgement

The authors would like to acknowledge the support from the Transportation Research and Injury Prevention Program (TRIPP) at the Indian Institute of Technology, Delhi, and the Volvo Research Education Foundation.

## References

- [1] U. Ackerman, *PDQ Physiology*, 2002. Available at <http://www.fleshandbones.com/readingroom/pdf/226.pdf>.
- [2] K. Bhalla, Y. Takahashi, J. Shin, C. Kam, D. Murphy, C. Drinkwater, and J. Crandall, *Experimental investigation of the response of the human lower limb to the pedestrian impact loading environment*, Proceedings of the Society of Automotive Engineer World Congress, Paper No. 2005-01-1877, 2005.
- [3] A. Chawla, S. Mukherjee, D. Mohan, and A. Parihar, *Validation of lower extremity model in THUMS*, Proceedings of the IRCOBI Conference, 2004, pp. 155–166.
- [4] A. Chawla, S. Mukherjee, A. Soni, and R. Malhotra, *Effect of active muscle forces on knee injury risks for pedestrian*

- standing posture at low speed impacts*, Proceedings of the IRCOBI Conference, 2007, pp. 95–112.
- [5] A.B. Chidester and R.A. Isenberg, *Final report – The pedestrian crash data study*, Proceedings of the 17th Enhanced Safety of Vehicle Conference, Paper No. 248, 2001.
- [6] J. Kajzer, S. Cavallero, J. Bonnoit, A. Morjane, and S. Ghanouchi, *Response of the knee joint in lateral impact: Effect of bending moment*, Proceedings of the IRCOBI Conference, 1993, pp. 105–116.
- [7] J. Kajzer, S. Cavallero, S. Ghanouchi, and J. Bonnoit, *Response of the knee joint in lateral impact: Effect of shearing loads*, Proceedings of the IRCOBI Conference, 1990, pp. 293–304.
- [8] J. Kajzer, H. Ishikawa, Y. Matsui, and G. Schroeder, *Shearing and bending effects at the knee joint at low speed lateral loading*, Proceedings of the Society of Automotive Engineer World Congress, Paper No. 1999-01-0712, 1999.
- [9] J. Kajzer, G. Schroeder, H. Ishikawa, Y. Matsui, and U. Bosch, *Shearing and bending effects at the knee joint at high speed lateral loading*, Proceedings of the Society of Automotive Engineer World Congress, Paper No. 973326, 1997.
- [10] J. Kerrigon, K. Bhalla, N. Madeley, J. Funk, D. Bose, and J. Crandall, *Experiments for establishing pedestrian impact lower injury criteria*, Proceedings of the Society of Automotive Engineers world Congress, Paper No. 2003-01-0895, 2003.
- [11] A.D. Kuo and F.E. Zajac, *A biomechanical analysis of muscle strength as a limiting factor in standing posture*, J. Biomech. 26 (1993), pp. 137–150.
- [12] K.W. Lia, H.H. Wub, and Y.C. Linb, *The effect of shoe sole tread groove depth on the friction co-efficient with different tread groove widths, floors and contaminants*, App. Eng. 37 (2006), pp. 743–748.
- [13] T. Maeno and J. Hasegawa, *Development of a finite element model of the total human model for safety (THUMS) and application to car-pedestrian impacts*, Proceedings of the 17th Enhanced Safety of Vehicle Conference, Paper No. 494, 2001.
- [14] Y. Matsui, *Biofidelity of TRL legform impactor and injury tolerance of human leg in lateral impact*, Stapp Car Crash J. 45 (2001), pp. 495–510.
- [15] Y. Mizuno, *Summary of IHRA pedestrian safety WG activities – Proposed test methods to evaluate pedestrian protection afforded by passenger cars*, Proceedings of the 18th Enhanced Safety of Vehicle Conference, Paper No. 580, 2003.
- [16] Y. Mizuno, *Summary of IHRA pedestrian safety WG activities-proposed test methods to evaluate pedestrian protection afforded by passenger cars*, Proceedings of 19th International Technical Conference on the Enhanced Safety of Vehicles, Paper No. 138, 2005.
- [17] K. Nagasaka, K. Mizuno, E. Tanaka, S. Yamamoto, M. Iwamoto, K. Miki, and J. Kajzer, *Finite element analysis of knee injury in car-to-pedestrian impacts*, Int. J. Traffic Inj. Prev. 4 (2003), pp. 345–354.
- [18] J.P. Schuster, C.C. Chou, P. Prasad, and G. Jayaraman, *Development and validation of a pedestrian lower limb non-linear 3-D finite element model*, Stapp Car Crash J. 44 (2000), pp. 315–334.
- [19] A. Soni, A. Chawla, and S. Mukherjee, *Effect of muscle active forces on the response of knee joint at low speed lateral impacts*, Proceedings of the Society of Automotive Engineers world Congress, Paper No. 2006-01-0460, 2006.
- [20] A. Soni, A. Chawla, and S. Mukherjee, *Effect of muscle contraction on knee loading for a standing pedestrian in lateral impacts*, Proceedings of the 20th Enhanced Safety of Vehicle Conference, Paper No. 467, 2007.
- [21] Y. Takahashi and Y. Kikuchi, *Biofidelity of test devices and validity of injury criteria for evaluating knee injuries to pedestrians*, Proceedings of the 17th Enhanced Safety of Vehicle Conference, Paper No. 373, 2001.
- [22] A.J. Vander, J.H. Sherman, and D.S. Luciano, *Human Physiology: The Mechanisms of Body Function*, Tata McGraw-Hill, New York, 1981.
- [23] A.M. Woodhull, K. Maltrud, and B.L. Mello, *Alignment of the human body in standing*, Euro. J. Appl. Physiol. 54 (1985), pp. 109–115.
- [24] World Bank Road Safety, 2001. Available at <http://www.worldbank.org/transport/roads/safety.html>.